Nonequilibrium electronic and structural Jahn-Teller dynamics in $(NbSe_4)_3I$

D. Dvorsek,[1] V. V. Kabanov,[1] K. Biljakovic,[2] and D. Mihailovic[1]
[1]*Jozef Stefan Institute, Jamova 39, Ljubljana, Slovenia*
[2]*Institute of Physics, Bijenicka 46, Zagreb, Croatia*
(Received 3 February 2006; revised manuscript received 26 May 2006; published 29 August 2006)

Femtosecond time-resolved optical spectroscopy reveals complex nonequilibrium electronic and structural relaxation dynamics associated with an electronically driven Jahn-Teller (JT) structural phase transition at 274 K in the quasi-one-dimensional semiconductor $(NbSe_4)_3I$. The relaxation dynamics of the electronic order parameter η (associated with the JT transition) and accompanying structural relaxation are described using the Landau-Khalatnikov equation, and equations of motion for coupled phonons, respectively.

DOI: 10.1103/PhysRevB.74.085211 PACS number(s): 73.21.−b, 78.47.+p, 73.20.Mf, 71.70.Ej

I. INTRODUCTION

Lattice dynamics often plays an important role in determining the functional properties of materials, but relatively little is known about the structural relaxation dynamics accompanying electronic ordering phenomena. Recent time-resolved studies using femtosecond optical spectroscopy of charge-density wave systems [both one-dimensional (1D) and 2D],[1,2] as well as systematic studies of cuprates,[3,4] MgB_2,[5] heavy fermion systems,[6] and manganites,[7] have given us a good phenomenological understanding of the relaxation dynamics of single particle excitations on the femtosecond time scale. However, while electron relaxation dynamics in functional electronic materials are relatively well understood,[1–8] there are no experimental techniques currently available which can give complementary structural dynamics information on short time scales. In an attempt to investigate the nonequilibrium *structural* dynamics which accompanies electronic relaxation, we decided to investigate the time-resolved optical response on the femtosecond time scale in a system where cooperative structural ordering is directly linked to the electronic degrees of freedom.

A classic example of electronically driven structural ordering occurs in $DyVO_4$,[9] where a nearly degenerate set of ground electronic levels ψ_1 and ψ_2 are mixed by a lattice vibration Q of appropriate symmetry resulting in a cooperative pseudo–Jahn-Teller effect, which in turn leads to long-range structural ordering.[10] An example of more recent interest, where functional properties arise from Jahn-Teller coupling between electronic levels and lattice modes are magnetoresistive manganites. However, the interplay between magnetic and Jahn-Teller (JT) structural ordering in these materials leads to rather complicated relaxation dynamics,[7] and the details of the spin, charge and lattice dynamics are not yet properly understood.[11]

To elucidate structural dynamics in a Jahn-Teller system without interference from magnetic ordering, we have performed a time-resolved femtosecond spectroscopy study of the nonmagnetic quasi-one-dimensional semiconductor $(NbSe_4)_3I$. This material displays a JT-driven structural phase transition at $T_c=274$ K, in which the structural reordering is accompanied by a change in band gap from $\Delta_{T>T_c}=100$ meV to approximately $\Delta_{T<T_c}\simeq 220$ meV below T_c (see inset to Fig. 2). We present real-time data on non-equilibrium single-particle electronic relaxation across the semiconducting band gap and measurements of the lattice relaxation dynamics (nonequilibrium phonons) associated with relaxation of coherently excited structural perturbations on the femtosecond time scale. The system is first perturbed by an ultrashort optical laser pulse, which excites electrons and holes, perturbing the electronic state. By virtue of the direct coupling between the charge and lattice degrees of freedom, the change in the population of the electronic ground state causes a coherent excitation of lattice phonons.[12,13] The oscillation of ions associated with the coherently excited phonons causes small modulations in the dielectric constant on the femtosecond time scale, which we can detect by time-resolved measurements of reflectivity. From such measurements we can deduce the decay kinetics of the electronic excitations, and independently, the dynamics of different coherently excited phonons in the system. Of course, we are particularly interested in those phonons which are coupled to the order parameter associated with the JT ordering transition. The results have a bearing on the understanding of the interplay between structural and electronic degrees of freedom of many other systems, particularly manganites and cuprates.

The structure of $(NbSe_4)_3I$ consists of $(NbSe_4)$ chains parallel to the c axis separated from one another by iodine atoms[14] (see Fig. 1). Within the chains, the Nb atoms alternate with Se_4 rectangles, which leads to an overlap of Nb $4d_{z^2}$ orbitals, giving the material a highly 1D character. Above T_c, the chains are strongly distorted and have two

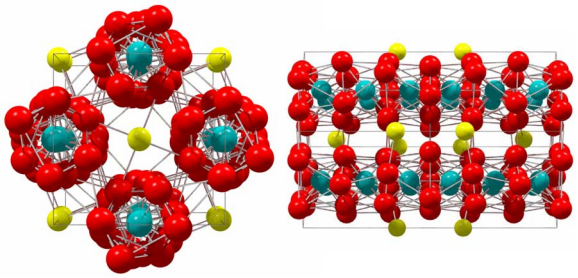

FIG. 1. (Color online) The structure of $(NbSe_4)_3I$ shown along the [001] and [110] axes, respectively. The Nd atoms are at the center of each chain and are surrounded by Se atoms. The I atoms are in between the chains.

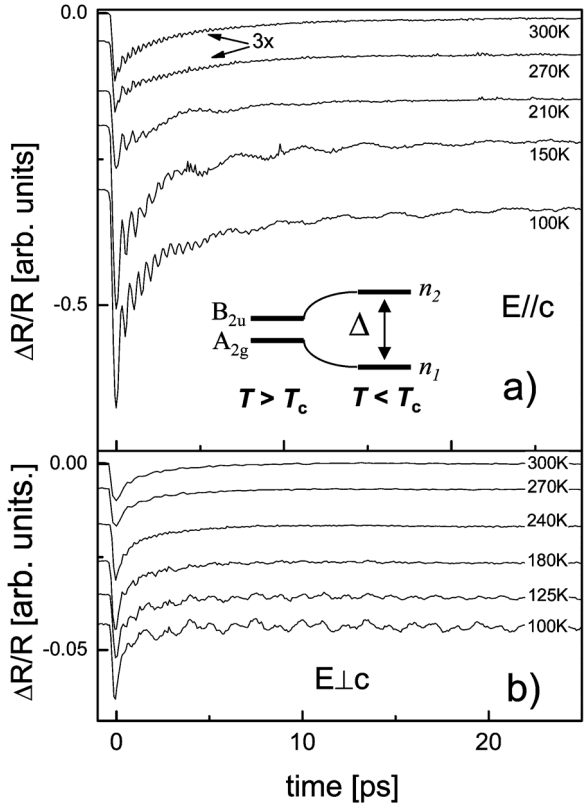

FIG. 2. The photoinduced reflection $\Delta R/R$ from $(NbSe_4)_3I$ at different temperatures as a function of time, measured (a) with the polarization of probe pulse in the direction parallel to the crystal axis c [the direction of $(NbSe_4)$ chains] and (b) perpendicular to the crystal axis c.

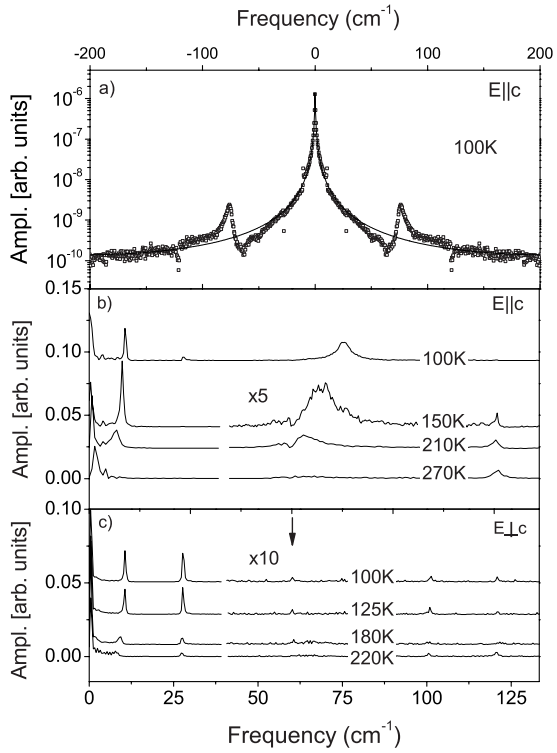

FIG. 3. (a) The fast Fourier transform of the photoinduced reflection $\Delta R/R$ data obtained with the probe polarization parallel to the chains. (Note the logarithm scale.) The solid line trough the data points (open squares) is the fit to the stretch exponential function made in the time domain. The phonon spectra at different temperatures obtained with (b) $E\|c$ and (c) $E\perp c$.

long Nb-Nb distances of 3.25 Å and a short Nb-Nb distance of 3.06 Å in the unit cell.[14] The coupling between the A_{2g}-symmetry valence band (VB) and the B_{2u} symmetry conduction band (CB) via a B_{1u} phonon results in a pseudo–Jahn-Teller instability which manifests itself in a structural rearrangement and an accompanying increase in the semiconducting gap.[15–18] Raman[18] and neutron[19] measurements showed a two phonon mode softenings as T_c was approached from below. Neutron measurements in particular suggested soft-mode behavior for a mode with a low-temperature frequency of 0.37 THz. At the phase transition, which is ferrodistortive but nonferroelectric, the space group changes from $P4/mnc$ (D_{4h}^4) above T_c to $P\bar{4}2_1c$ (D_{2d}^4) below T_c. Below T_c the spontaneous structural deformation appears, and the chains are less distorted with Nb-Nb distances of 3.31, 3.17, and 3.06 Å, respectively.[20] Below T_c the point group does not have a center of inversion, and infrared active modes become Raman active. Above T_c the electronic order parameter for the JT transition η is defined as $\eta=\langle\psi_{A_{2g}}^*\psi_{B_{2u}}+\psi_{B_{2u}}^*\psi_{A_{2g}}\rangle$, where $\psi_{A_{2g}}$ and $\psi_{B_{2u}}$ are the VB and CB electronic wave functions, respectively. Below T_c the *difference* in occupancy n_1-n_2 of the VB and CB is directly related to the order parameter η. This has the important consequence that a short laser pulse which can excite electrons from the VB into the CB (directly or indirectly) will also drive the lattice into a nonequilibrium state via the JT coupling. The relaxation of the electronic subsystem can be studied in real time by monitoring the time dependence of the photoinduced reflectivity—which is directly related to the nonequilibrium difference in carrier density n_1-n_2.[3] The structural relaxation dynamics can be monitored by detecting the relaxation of coherent phonon oscillations of totally symmetric phonon modes, all of which are directly coupled to the order parameter η below T_c.

II. EXPERIMENTAL RESULTS

The time-resolved reflectivity measurements were performed by first exciting the material using the pump-probe technique where the small change of reflectivity $\Delta R/R$ caused by a pump laser pulse is detected by a suitably delayed weak probe pulse.[1–6] Here an amplified Ti:sapphire laser was used at 800 nm and pulse lengths of $\tau_p \approx 80$ fs for both pump and probe light pulses at a repetition rate of 250 kHz. The typical energy of pump pulses was 12 nJ and an intensity ratio of pump and probe pulses was approximately 100:5. The diameter of the beams was ~ 100 μm and the crystal surface was parallel to the ac crystal plane. All the temperature-dependent measurements were performed in the heating part of the temperature cycle.

The photoinduced (PI) reflection $\Delta R/R$ of a $(NbSe_4)_3I$ single crystal as a function of time is shown in Fig. 2 for different T. The measurements were done with polarization

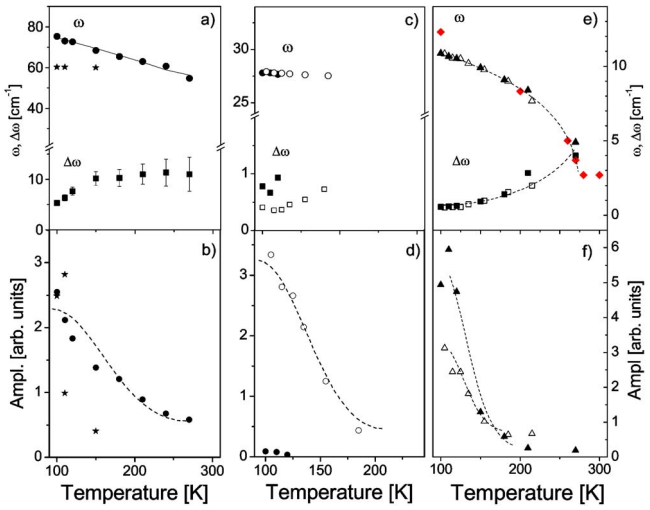

FIG. 4. (Color online) (a) The T dependence of ω of the 80 and 60 cm^{-1} mode (circles and stars, respectively), and linewidth $\Delta\omega$ of the 80 cm^{-1} mode (squares). (b) Amplitude of the 80 (circles) and 60 cm^{-1} (stars) modes, respectively (c) The frequency and linewidth and (d) the amplitude of the 27 cm^{-1} mode. The polarization dependence of the linewidth (c) and amplitude (d) is unusual: filled symbols are for $E\|c$, while open symbols are for $E\perp c$. (e) ω and $\Delta\omega$ of 12 cm^{-1} mode. Full triangles for $E\|c$ and open triangles for $E\perp c$. The neutron data (Ref. 19) are also shown by red diamonds. (f) Amplitude of the 12 cm^{-1} mode.

of probe pulses either along the ($NbSe_4$) chains ($E\|c$), or perpendicular to the chains ($E\perp c$). We can clearly see oscillatory decaying components due to coherently excited phonons, superimposed on an exponential decay, both being strongly T dependent. To analyze the different components of the photoinduced reflection $\Delta R/R$ in frequency domain we perform a fast Fourier transform of the data, shown in Fig. 3. To analyze the phonons in detail, we subtract the central peak (which arises from the electronic single-particle relaxation), which will be analyzed separately.

Comparing the spectra [Fig. 3(b)] with published Raman data,[18,21] we see remarkable advantages of increased spectral range at low frequency, significantly improved resolution and much-improved signal-to-noise ratio of the present technique, which is particularly important for the study of low frequency excitations. Of particular interest is the fact that at T_c the crystal loses its center of inversion, and several modes which were of B_{1u} symmetry above T_c become Raman active below T_c and therefore all of them may be observed by time domain spectroscopy independently of the polarization of the pump and the probe.[13] Our spectra for probe polarization $E\|c$ agree well with the polarized Raman spectra obtained in $a'(cc)\bar{a}'$ geometry, and $E\perp c$ spectra are in agreement with $a'(b'b')\bar{a}'$ Raman spectra. In Fig. 3(b) we can see a mode at around 80 cm^{-1} which strongly softens and broadens with increasing temperature approaching T_c. Remarkably, it also exhibits a clear Fano resonance dip when it crosses a mode at 60 cm^{-1}. This 60 cm^{-1} mode is not clearly evident in Fig 3(b) for $E\|c$, but is seen as a very sharp mode in $E\perp c$ probe polarization [Fig. 3(c)]. This Fano interference was already noted previously.[21] However, the suggestion by Sekine *et al.*[19,21] of anticrossing behavior—whereby the frequency of the higher frequency phonon mode becomes fixed, while the lower frequency mode behaves as a soft mode—is not confirmed by the present experiments. Rather, it appears that the mode simply becomes overdamped as $T\rightarrow T_c$. Turning our attention to the low-frequency range, we observe that the frequency of the mode at 28 cm^{-1} is virtually T independent, while the 12 cm^{-1} mode (B_{1u} symmetry above T_c) exhibits strong softening as $T\rightarrow T_c$. The temperature dependence of the ω, linewidth $\Delta\omega$, and amplitude of the observed modes is shown in Fig. 4. We note that the mode at 80 cm^{-1} cannot be designated as a proper soft mode, as it remains at 60 cm^{-1} at $T=T_c$. The 12 cm^{-1} phonon softens substantially as T_c is approached and becomes critically damped above 250 K, such that $\Delta\omega\simeq\omega$. As already stated, all the observed modes are fully symmetric below T_c, consistent with coherent phonon mechanism.[12,13]

We now turn to an analysis of the nonoscillatory relaxation which is the result of the large photoinduced reflectivity transient (Fig. 2). To fit the time-domain data we use a stretch exponential function of the form $\Delta R(t,T)/R = A(T)\exp\{-[t/\tau_A(T)]^{\mu}\}$. The fit is shown to be very good with $\mu=0.4$ as can also be seen in its Fourier transform [Fig. 3(a)]. We have also tried to fit the data with the sum of two exponentially decaying functions but the fits were significantly worse. The temperature dependence of $\tau_A(T)$ for both $E\|c$ and $E\perp c$ of probe pulses and the amplitude $A(T)$ with $E\|c$ are shown in Fig. 5. We first notice that temperature dependence of the amplitude and decay kinetics of this component is remarkably similar to that observed in superconductors and other materials with a soft gap (or pseudogap). Usually this dynamics is attributed to the relaxation of nonequilibrium quasiparticle density.[3–8] Therefore we attribute this component to the relaxation of nonequilibrium quasiparticles across the gap, associated with the relaxation of the electronic order parameter η. The T dependence is seen to fit well with the predictions of Kabanov's model for the T dependence of the photoinduced quasiparticle density:[3]

$$\Delta R(t,T)/R = \frac{E_l/[E_g(T)+k_BT]}{1+\Lambda\sqrt{4k_BT/\pi E_g(T)}\exp[-E_g(T)/2k_BT]},$$

where the coefficient Λ depends on the number of modes interacting with the quasiparticles and the density of states near Fermi energy. We have assumed a mean-field-like temperature dependence of the energy gap $E_g(T) = \Delta_0\sqrt{(1-T/T_c)}+\Delta_{T>Tc}$. The value of gap obtained in the fit is close to that obtained by other techniques[18] and unambiguously confirms our assignment of the nonoscillatory relaxation component of the reflectivity transient as an electronic order parameter.

III. DISCUSSION AND CONCLUSIONS

We can clearly see in Fig. 2 that the time evolution of $\Delta R/R$ cannot be attributed to the damped oscillations of the order parameter (soft mode) which would be of the form $e^{-t/\tau}\cos(\omega t+\phi)$. The implication is that in spite of the soft-mode-like behavior, the 12 cm^{-1} B_{1u} mode is actually *not* the

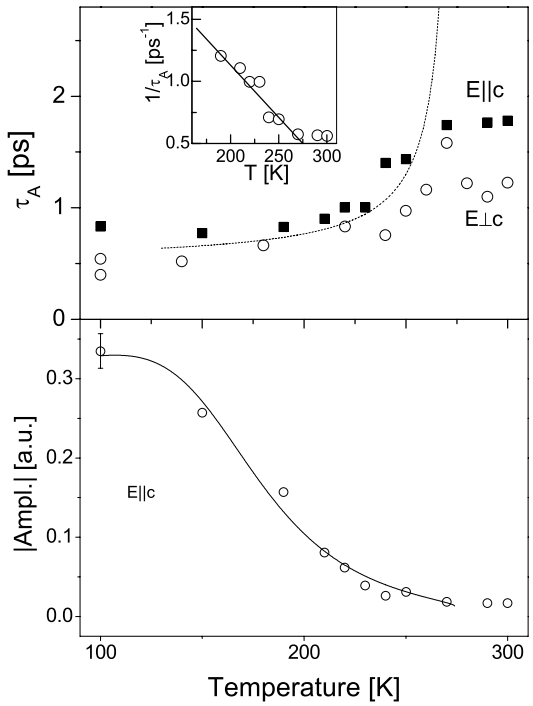

FIG. 5. The temperature dependence of the nonoscillatory component of photoinduced signal. (a) The two relaxation rates $1/\tau_A$ for the two directions of probe pulses polarization at different temperatures and (b) the temperature dependence of the corresponding amplitudes $A(T)$. The solid line in $E\|c$ polarization is a fit using Kabanov's model (Ref. 3). The parameters are $\Lambda\sqrt{2/\pi}=200$, $\Delta_{T<T_c}=58$, 6 meV (680 K), $\Delta_0=113$ meV (1492 K).

soft mode for the transition as previously thought.[19] Rather, an order-disorder type electronic phase transition takes place, described by the order parameter η, to which phonon modes of appropriate symmetry (such as the 12 cm^{-1} mode) are coupled. Therefore we apply the theory of bilinear coupling with the soft mode coordinate in the similar way as it was discussed in Ref. 22. The Landau functional can then be written in terms of the order parameter η and coupled phonon displacement Q:

$$F = \frac{\alpha}{2}(T - T_{c0})\eta^2 + \frac{\beta}{4}\eta^4 + \gamma\eta Q + \frac{d}{2}Q^2,$$

here α, β, γ, and d are temperature independent constants, and T_{c0} is the unrenormalized critical temperature. The phase transition occurs at $T_c = T_{c0} + \gamma^2/\alpha d$ and at equilibrium $\eta_0 = \sqrt{\alpha(T_c - T)/\beta}$ is proportional to static deformation $Q_0 = (-\gamma/d)\eta_0$. After photoexcitation, the fluctuations $\Delta\eta = \eta - \eta_0$ and $\Delta Q = Q - Q_0$ satisfy the following coupled rate equations for $\Delta\eta$ and ΔQ: $\Delta\dot{\eta} = -\varkappa(\kappa\Delta\eta + \gamma\Delta Q)$; $\Delta\dot{Q} + \lambda\Delta Q = -\chi(\gamma\Delta\eta + d\Delta Q)$, where, $\varkappa$, χ, and λ are kinetic coefficients and $\kappa = 2\alpha(T_c - T) + \gamma^2/d$. Since $\Delta R \propto \eta_0(\Delta\eta + \text{const}\,\Delta Q)$ the time evolution of the photoinduced reflection can be written as[23]

$$\Delta R(t,T) \propto \eta_0[e^{-t/\tau_A} + Ke^{-t/\tau_B}\cos(\Omega t - \varphi)], \qquad (1)$$

independent of initial conditions. Here K and ϕ are temperature independent constants

$$\tau_A^{-1} = 2\alpha\Omega_0^2\varkappa(T_c - T)/(\lambda\varkappa\gamma^2/d + \Omega_0^2), \qquad (2)$$

$\Omega_0^2 = d\chi$ is phonon frequency well above T_c. τ_B and renormalized phonon frequency Ω are weakly temperature dependent and can be expressed analytically at $T = T_c$ $\tau_B^{-1} = (\lambda + \varkappa\gamma^2/d)/2$, $\Omega = \sqrt{\Omega_0^2 - (\tau_B^{-1} - \varkappa\gamma^2/d)^2}$. Equation (1) describes coherent oscillations with temperature dependent frequency Ω and damping τ_B^{-1} superimposed on the exponential relaxation of the order parameter. The electronic relaxation time τ_A is expected to show critical behavior, diverging as $T \to T_c$.

The amplitudes of both phonon modes [Figs. 4(b) and 4(f)] are decreasing near T_c, qualitatively as predicted by Eq. (1). The width $1/\tau_A$ of the central peak shown in Fig. 5(a) decreases approximately linearly on approaching T_c from below, which agrees well with the critical behavior described by Eq. (2). The same expression also predicts a decrease of amplitude of the central peak close to T_c, which is also clearly observed in Fig. 5(b). The simplified model given above thus captures the main observations associated with the JT phase transition at 274 K presented in Fig. 2, such as the fact that the amplitudes of the nonoscillatory and oscillatory parts decay as $T \to T_c$, and the phonon frequencies and relaxation times τ_B of the oscillations become temperature dependent due to interaction with the order parameter η.

The analysis of the new data from time-resolved optical spectroscopy shows a clear link between the structural and electronic relaxation phenomena accompanying the electronically driven Jahn-Teller transition at 274 K. From the data we measure the relaxation of the electronic order parameter η in real time, and determine how structural displacements follow the electronic relaxation. The behavior of both structural ordering and electronic relaxation can be described using a Landau-Khalatnikov equation for the relaxation of the order parameter (soft mode) coupled to vibrations of appropriate symmetry.

The electronic relaxation associated with an increase in the band gap below 274 K in $(NbSe_4)_3I$ has a remarkably similar temperature dependence to the single-particle relaxation across the so-called pseudogap at T^* in superconducting cuprates.[3,4] Both are related to single particle relaxation across a semiconducting and pseudogap, respectively. On the other hand, a similar increase in the phonon intensity below T_c arising from a change in symmetry below T_c in $(NbSe_4)_3I$ is observed in cuprates where certain infrared-active phonons become Raman active below T^*.[24–26] The major difference between the two types of system appears to be that long-range cooperative JT ordering is present in $(NbSe_4)_3I$, while in the high-temperature superconductor only dynamic local structural deformations[27] below T^* have been reported. Different types of structural effects in the two types of systems are also highlighted by the fact that mean-field-like phonon mode softening associated with long-range cooperative structural ordering is not observed in cuprates.

ACKNOWLEDGMENTS

We thank H. Berger and F. Levy for providing the samples which have been synthesized at EPFL, Lausanne and P. Monceau for valuable discussions.

[1] J. Demsar, K. Biljakovic, and D. Mihailovic, Phys. Rev. Lett. **83**, 800 (1999).
[2] J. Demsar, L. Forro, H. Berger, and D. Mihailovic, Phys. Rev. B **66**, 041101(R) (2002).
[3] V. V. Kabanov, J. Demsar, B. Podobnik, and D. Mihailovic, Phys. Rev. B **59**, 1497 (1999).
[4] V. V. Kabanov, J. Demsar, and D. Mihailovic, Phys. Rev. B **61**, 1477 (2000); J. Demsar, B. Podobnik, V. V. Kabano, Th. Wolf and D. Mihailovic, Phys. Rev. Lett. **82**, 4918 (1999); C. J. Stevens, D. Smith, C. Chen, J. F. Ryan, B. Podobnik, D. Mihailovic, G. A. Wagner, and J. E. Evetts, *ibid.* **78**, 2212 (1997).
[5] J. Demsar, R. D. Averitt, A. J. Taylor, V. V. Kabanov, W. N. Kang, H. J. Kim, E. M. Choi, and S. I. Lee, Phys. Rev. Lett. **91**, 267002 (2003).
[6] J. Demsar, R. D. Averitt, K. H. Ahn, M. J. Graf, S. A. Trugman, V. V. Kabanov, J. L. Sarrao, and A. J. Taylor, Phys. Rev. Lett. **91**, 027401 (2003).
[7] T. Mertelj, D. Mihailovic, Z. Jaglicic, A. A. Bosak, O. Yu. Gorbenko, and A. R. Kaul, Phys. Rev. B **68**, 125112 (2003).
[8] D. Mihailovic, D. Dvorsek, V. V. Kabanov, J. Demsar, L. Forro, and H. Berger, Appl. Phys. Lett. **80**, 871 (2002); D. Dvorsek, V. V. Kabanov, J. Demsar, S. M. Kazakov, J. Karpinski, and D. Mihailovic, Phys. Rev. B **66**, 020510(R) (2002).
[9] R. J. Eliott, R. T. Harley, W. Hayes, and S. R. P. Smith, Proc. R. Soc. London, Ser. A **328**, 217 (1972), and references therein. For a review of theoretical discussion see G. A. Gehring and K. A. Gehring, Rep. Prog. Phys. **38**, 1 (1975).
[10] E. Pytte and K. W. H. Stevens, Phys. Rev. Lett. **27**, 862 (1971); B. Halperin, Phys. Rev. B **7**, 894 (1972).
[11] R. D. Averitt, A. I. Lobad, C. Kwon, S. A. Trugman, V. K. Thorsmolle, and A. J. Taylor, Phys. Rev. Lett. **87**, 017401 (2001).
[12] H. J. Zeiger, J. Vidal, T. K. Cheng, E. P. Ippen, G. Dresselhaus, and M. S. Dresselhaus, Phys. Rev. B **45**, 768 (1992).
[13] T. E. Stevens, J. Kuhl, and R. Merlin, Phys. Rev. B **65**, 144304 (2002).
[14] A. Meerschaut, P. Palvadeau, and J. Rouxel, J. Solid State Chem. **20**, 21 (1977).
[15] N. Kristoffel and P. Konsin, Phys. Status Solidi **29**, 731 (1968).
[16] P. Gressier, A. Meerschaut, L. Guemas, J. Rouxel, and P. Monceau, J. Solid State Chem. **51**, 141 (1984).
[17] M. Izumi, T. Iwazumi, K. Uchinokura, R. Yoshizaki, and E. Matsuura, Solid State Commun. **51**, 191 (1984).
[18] T. Sekine and M. Izumi, Phys. Rev. B **38**, 2012 (1988).
[19] P. Monceau, L. Bernard, R. Currat and F. Levy, Physica B **156**, 20 (1989).
[20] P. Gressier, L. Guemas, and A. Meerschaut, Mater. Res. Bull. **20**, 539 (1985).
[21] T. Sekine, K. Uchinokura, M. Izumi, and E. Matsuura, Solid State Commun. **52**, 379 (1984).
[22] V. L. Ginzburg, A. A. Sobyanin, and A. P. Levanyuk, *Light Scattering Near Phase Transition*, edited by H. Z. Cumins and A. P. Levanyuk (North Holland, Amsterdam, 1983).
[23] D. Dvorsek, Ph.D. Thesis, Faculty of Mathematics and Physics, University of Ljubljana, Ljubljana, 2005.
[24] O. V. Misochko, E. Ya. Sherman, N. Umesaki, K. Sakai, and S. Nakashima, Phys. Rev. B **59**, 11495 (1999).
[25] O. V. Misochko, N. Georgiev, T. Dekorsy, and M. Helm, Phys. Rev. Lett. **89**, 067002 (2002).
[26] V. V. Kabanov and D. Mihailovic, Phys. Rev. B **65**, 212508 (2002).
[27] T. Egami and S. J. L. Billinge, *Underneath the Bragg Peaks, Structural Analysis of Complex Materials*, Vol. 7 of *Pergamon Materials Series* (Elsevier, Amsterdam, 2003).